An Effective Power and Performance Control in Translucent Network with GMPLS Control Plane

[1]A.Abitha, [2] A.Jothi, [3] T.Nagajothi, [4] M.Sudha, [5]R.Padmanaban
[1,2,3,4] UG Scholar, Mangayarkarasi college of Engineering, Madurai
[5] Assistant Professor, Mangayarkarasi college of Engineering, Madurai

Abstract-In this paper; we labeled the optical power adaptation in translucent optical networks. We extended the GMPLS protocol suite in order to carry optical regeneration and the power adaptation process. In this respect, a Track Computation Algorithm with new protocol extensions and signaling mechanisms was proposed to RSVP-TE & OSPF-TE protocols. These extensions allow taking into account the optical regenerator availability and assignment as well as performing channel power adaptation using particle swarm optimization (PSO). Moreover, the migration from fixed-grid to flexible-grid networks was studied with dynamic traffic patterns, where it was demonstrated that the power saturation problem. Moreover, including all flexibility parameters (such as baud rate, modulation format, and others) in the routing algorithm would improve the usage of network resources. This increases its capacity and could even increase the optical power issue.

.

Keywords—Flex-grid; GMPLS; Optical power control; Optical regeneration; OSNR margins; OSPF-TE; RSVP-TE.

I. INTRODUCTION

The evolution to translucent optical networks was driven by the scalability problem of transparent net-works where optical impairments limit the reach of optical connections. This is usually the case for large networks, where optical channels suffer from the accumulation of optical impairments when undergoing a high number of optical links. Indeed, the deployment of optical regenerators allows us to overcome the signal degradation experienced over network links and thus guarantees a feasible channel between any two optical nodes. However, the use of optical regenerators increases the complexity of channel provisioning, where additional information is required by the path computation algorithm to assign regeneration sites. Therefore, establishing such channels requires extensions to control the plane protocols in order to take into account the regeneration information during the path computation and signaling phase.

In our previous work [1], the migration from fixed-grid to flex-grid networks has been studied only for transparent networks with an incremental traffic pattern. The proposed power adaptation process and protocol extensions have considered channel provisioning without regeneration information. In a continuation of what has already been studied, in this paper we address the migration from fixed-grid to flex-grid for the case of translucent networks that are representative of current networks. Furthermore, as the next generation of optical networks is intended to be flexible and dynamic, we consider in this work dynamic traffic scenarios, where optical channels are dynamically established and removed without a prior knowledge of the traffic re-quests. In this respect, the impact of the power saturation problem is evaluated considering this kind of traffic pattern.

II. STATE OF THE ART

In the literature, several works [2–5] have addressed the establishment of optical channels in translucent optical networks, where signaling mechanisms and protocol extensions were proposed to handle the optical regeneration in the generalized multi-protocol label switching (GMPLS) control plane. Indeed, as with the optical impairments [6], different approaches (i.e., routing-based or signaling-based) can be developed to take into account the optical regeneration information in the control plane. These ap-proaches are usually based on the open shortest-path-first traffic engineering (OSPF-TE) and resource-reservation-protocol traffic engineering (RSVP-TE) protocols. This consists of adding new extensions to include the required information, such as regenerator availability and regenerator reservation information.

The works in Refs. [2,3] have proposed novel extensions to the OSPF-TE protocol to enable the dissemination of optical regeneration information (e.g., the availability of regenerators' modules, regeneration types: 1R, 2R, 3R [7]).

These extensions allow for optical nodes, being aware of the number, the type, and the location of available regenerators in the network. Moreover, the authors proposed adding a new sub-object called a regenerator sub-object in the explicit route object (ERO) of the RSVP-TE Path message. This extension was added in order to specify the optical regenerators that should be used during the signaling phase when establishing an optical channel.

In Ref. [4], the authors proposed several extensions to RSVP-TE and OSPF-TE protocols to take into account optical regeneration in the GMPLS control plane. The OSPF-TE extensions were proposed to advertise the information on regenerator availability and capability (i.e., number of re-generators per node and regeneration types). The RSVP-TE extensions were used to collect regenerator information and assign regenerators along the connection path. In this respect, the authors proposed three extensions to the RSVP-TE protocol: a regenerator object (RO), a regenerator flag (RF), and a regenerator availability object (RAO). In brief, the RO extension was used to assign the regenerator to be used (i.e., by handling the regenerator ID). The RF extension was used to specify the optical node where regeneration should be performed. Finally, the RAO extension was used to collect the set of available regenerators in each intermediate node along the optical path. Therefore, depending on the information stored in the optical nodes, the information disseminated by OSPF-TE and the information to be collected by RSVP-TE (i.e., depending on the extensions used from the three proposed kinds), different provisioning strategies were proposed

[4]. Some are based only on RSVP-TE [8,9] in order to avoid the advertisement of a large amount of information in the control plane. Others are based on both protocols (i.e., RSVP-TE and OSPF-TE) [10].

Alternatively, in Ref. [5], a bit is appended in the wave-length label ERO sub-object, where it is used to indicate for intermediate nodes that an optical regeneration is required locally. This proposition considers that regenerator per node availability is already disseminated through the OSPF-TE protocol.

It is important to note that, in the literature, the case of a dynamic traffic pattern has never been considered previously for the case of power adaptation. All papers considering the power adaptation and other flexibility parameters use integer linear programming (ILP) algorithms with offline provisioning [11–13].

III. Contributions

To ensure interoperability in optical networks, it is important to respect networking protocol standards. Therefore, the achievement of any function should be com-pliant with specifications; otherwise, this may raise inter-operability issues with other networks. In this respect, the RSVP-TE extensions proposed in Refs. [4,5] do not respect the request for comments (RFC) standard of the RSVP-TE protocol, since non-standardized objects (e.g., RAO, RO) were defined and used to convey regeneration information rather than using standardized objects. On the contrary, the extensions proposed in Refs. [2,3] for RSVP-TE and OSPF-TE respect the RFC standards of these protocols. However, these extensions were proposed before the apparition of the RFC7581 and RFC7689 standard [14,15] in June and November 2015, respectively. Therefore, some of the encoding formats of these extensions should be adapted to the proposed standard.

Indeed, the RFC standard in Ref. [14] proposes specific encoding formats for a set of information fields described in Ref. [16]. These encoding formats concern information needed by the routing and wavelength assignment algorithm and are used to disseminate four categories of information: node information, link information, dynamic node information, and dynamic link information. The goal is to facilitate the path computation and the establishment of label switched paths (LSPs) in translucent optical networks.

In this paper, we focus on the node information that concerns optical regeneration modules and the connectivity matrix in optical nodes. However, we assume that there are no connectivity constraints in the optical nodes. Thus, only the information related to the optical regeneration modules is required to allow the assignment of the optical regeneration modules during the signaling of an optical channel. In this respect, we propose a new routing algorithm, a signaling mechanism, and protocol extensions for the GMPLS control plane to allow performance of the power adaptation process in translucent networks. In particular, we propose new extensions to the RSVP-TE and OSPF-TE protocols to take into account regeneration and power information during the establishment of a re-generated optical channel. The performance of the novel scheme is demonstrated with simulations considering dynamic traffic patterns. The simulated scenarios are evaluated through their blocking probability as a function of the network load under consideration.

Note that we are the first, to our knowledge, to present how the standardized regeneration extensions can be used in real implementation. Moreover, we are the first to pro-pose protocol extensions to deal with the power adaptation of optical channels.

The rest of this chapter is organized as follows. Section IV presents the method used to assign regeneration sites and the one used to compute the power adaptation coefficients for a regenerated optical path in a translucent network. Section V presents the developed routing algorithm that takes into account optical regeneration. Section VI is dedicated to the proposed extensions for the OSPF-TE and RSVP-TE protocols. The novel signaling mechanism is explained through an example of channel establishment. Section VII presents simulated scenarios and performance results over the considered network topology. Finally, the conclusion is presented in Section VIII

IV. Optical Power Control With Regeneration

A. Optical Regeneration Assignment Method

In translucent networks, when an optical channel is not physically feasible, an optical regeneration (for our purposes, an optical-to-electrical-to-optical conversion) is performed in one or several nodes along the path to get an acceptable quality of transmission at the receiver side. This quality of transmission can be represented through different parameters such as optical signal-to-noise ratio (OSNR), bit error rate (BER), or Q Factor. The OSNR is considered for this study.

Usually, the strategy of operators is to reduce the cost of the network by minimizing the number of regenerators used. This minimum cost is ensured by exploiting the maxi-mum reach of the optical transceivers. In this work, we consider this regeneration strategy, which we call hereafter the Traditional Regeneration Algorithm.

Figure 1 shows an example of connection establishment over an unfeasible optical path. In fact, the unfeasibility of the optical path requires the assignment of regeneration sites at intermediate nodes to get a working channel. In this example, several combinations for regeneration sites are possible; however, only one combination guarantees a minimum cost. Indeed, the regeneration combinations, such as regeneration in node A and C or regeneration in node A, B, and C, are possible, but they are not the best solution in terms of cost. Therefore, if the Traditional Regeneration Algorithm is applied, only node B is assigned to perform the optical regeneration, since it allows exploitation of the maximum reach of the transceiver and thus minimization of the number of regenerators used

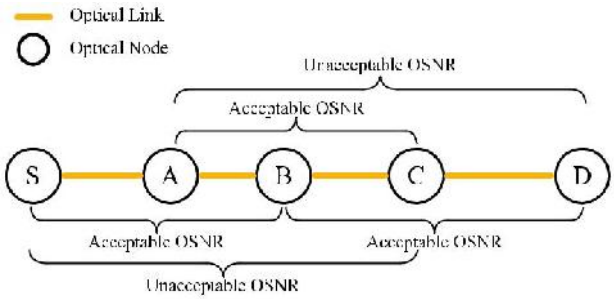

Fig. 1. Example of an unfeasible optical path between nodes S and D.

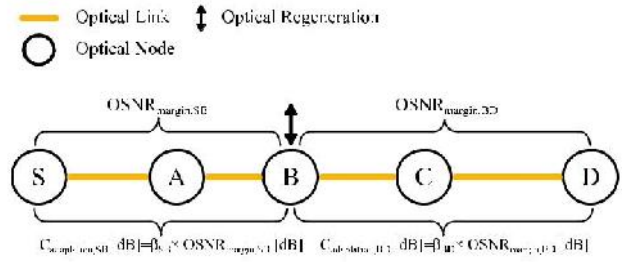

Fig. 2. Regeneration assignment using the Traditional Regeneration Algorithm.

B. Power Adaptation With Optical Regeneration

Once the regeneration sites are identified with any re-generation algorithm (e.g., the Traditional Regeneration Algorithm or another), the optical path is then decomposed into a set of feasible transparent segments. In Ref. [1], we proposed a power adaptation process to convert the OSNR margins ($OSNR_{margin}$) into optical power attenuation over optical links. To this end, a variable called the power adaptation coefficient ($C_{adaptation}$) was proposed. This coefficient represents the maximum power attenuation that can be applied for an optical channel between the source and destination nodes. Therefore, in order to perform the power adaptation process over the regenerated optical path, the power adaptation coefficient $C_{adaptation}$ should be computed for every transparent segment.

In this respect, OSNR estimation [1] is performed over each segment to compute the $OSNR_{margin}$ per segment and thus deduce the applicable $C_{adaptation}$ coefficient. Note that in Ref. [1], we defined $OSNR_{margin}$ as the difference between the minimum acceptable OSNR ($OSNR_{req}$) and the estimated one and $C_{adaptation}$ as the value of power attenuation that corresponds to $OSNR_{margin}$ for an optical channel.

Let us consider the example of Fig. 2, where an optical regeneration is performed in Node B. In this example, the optical path is decomposed into two transparent segments (SB and BD). Therefore, two $C_{adaptation}$ coefficients are computed using the two estimated $OSNR_{margin}$ values. Then, a channel power adaptation is applied at the transmitter side of each segment using the computed coefficients.

Note that $\beta \in 0, 1$ and is used by the control plane to introduce flexibility to the channel power adaptation. β indicates the portion of $OSNR_{margin}$ used per channel (consequently, the remaining $OSNR_{margin}$). This offers important flexibility for the control plane, where $OSNR_{margin}$ can be shared between different flexible parameters (such as optical power, modulation format, etc.). In this paper, we always set β 1 to maximize the optical power attenuation per channel and because optical power is the only variable parameter considered.

V. Routing Algorithm With Regeneration

To provision an optical channel in a translucent optical network, we propose a new Path Computation Algorithm that considers spectral and power resources, physical feasibility of the optical channel, and assignment of regenerations in addition to channel power adaptation. Figure 3 shows a simplified representation of the algorithm.

In this respect, the executed algorithm first computes the shortest path, using Dijkstra's Algorithm, for any optical connection request of T Gbit/s capacity, between a pair of source and destination nodes. Then, using the first-fit algorithm, it tries to find a group of S available slots of 12.5 GHz width each that are continuous, contiguous, and satisfy the capacity T of the request. For any request, the S slots are computed to get minimum spectrum occupation, supposing a fixed modulation format and baud rate. If no available slots are found, the connection request is blocked.

Furthermore, once the S available and successive spectrum slots over the shortest path p are found, the physical feasibility test is performed using the proposed OSNR estimator in Ref. [1]. This test checks whether an optical channel can be established transparently over path p (i.e., $OSNR_{est,p} > OSNR_{req,p}$). If that is the case, then a transparent segment can be established and just one $C_{adaptation}$ coefficient, at the source node, is required to adapt the power of the channel. In contrast, if the path is not physically feasible, one or several optical regenerations should be selected to get a working channel. The number of the regeneration sites depends on the accumulated impairments over the path and on the used regeneration assignment strategy (i.e., minimum number of regenerations or other strategies [17]). As a result, depending on the number of regeneration sites, path p is decomposed into a set of X transparent segments. Therefore, an $OSNR_{margin}$ is to be computed per segment to get the applicable $C_{adaptation}$ value.

After the computation of the $C_{adaptation}$ coefficients, a power verification test is performed to ensure that the newly added channel will not cause any saturation problems over the links constituting path p. This test consists of comparing, for every link of path p, the aggregate power P t (after adding the power of the new channel $P^{adapted}_{channel,l}$) with the maximum allowed one ($P_{max,l}$). We recall here that $P^{opt}_{channel,l}$ corresponds to the optimal optical power per channel over the link l [1], and $P^{adapted}_{channel,l}$ is the optical power of the same channel after applying the adaptation coefficient.

In the case where no optical regeneration is performed, the channel power value per link l is $P^{adapted}_{channel,l}$ $P^{opt}_{channel,l}/C_{adaptation,p}$. Contrariwise, in the case where optical regeneration is performed, a different $C_{adaptation}$ coefficient is applied per transparent segment.

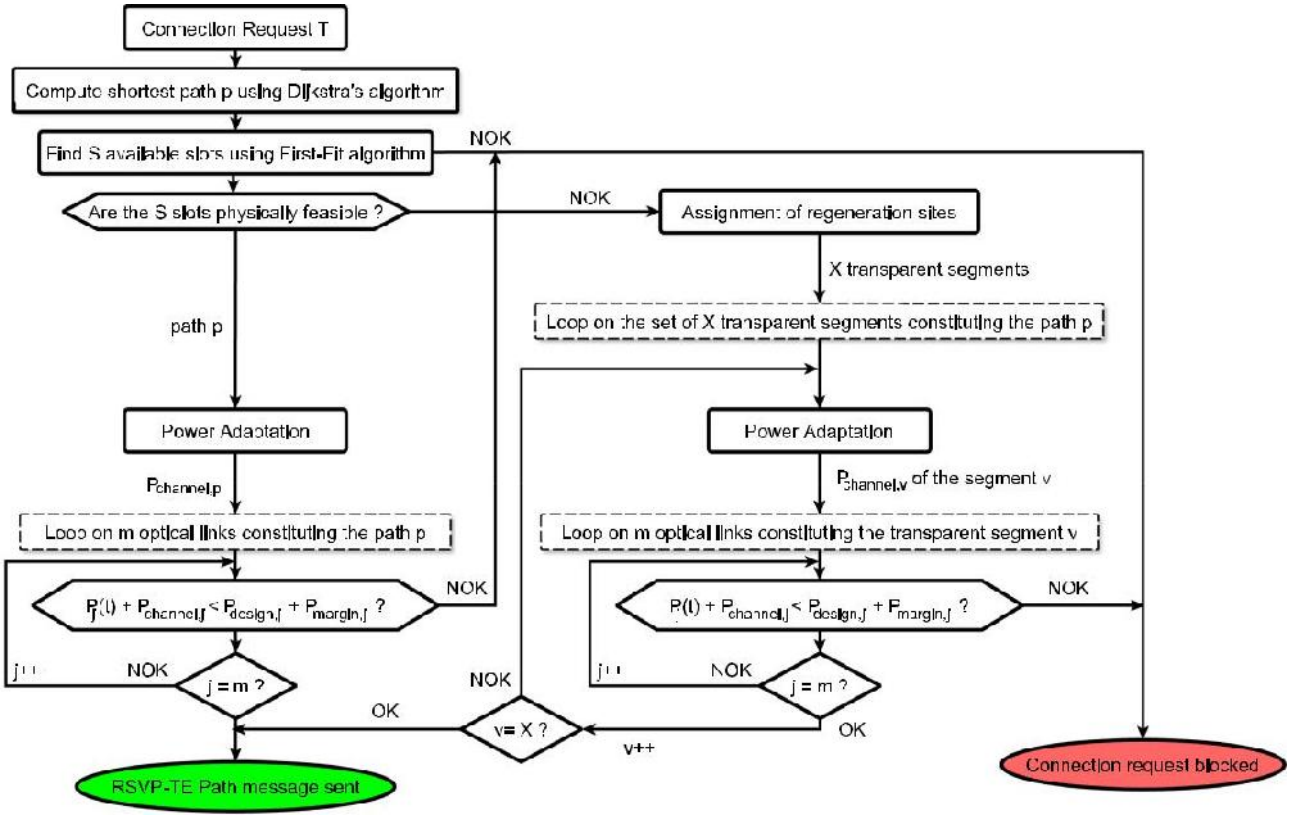

Therefore, the channel power value per link l is $P^{adapted}_{channel,l}$ $P^{opt}_{channel,l}/C_{adaptation,v}$, where v is the index of the transparent segment of path p. Once these tests are done, the signaling process can be triggered over the chosen path. In that case, an extended RSVP-TE Path message containing power and regeneration information is sent downstream in order to set up the optical channel. If any of these tests fail, the connection request is rejected.

Finally, in each crossed optical node during the signaling process, the power verification test is performed to check if the aggregated power over the outgoing link does not ex-ceed the $P_{max\ ,l}$. Indeed, if connection requests are frequent, some signaling processes may simultaneously compete for the same optical resources in terms of optical power (race condition). This is why the signaling should avoid any over-provisioning due to the not-yet-updated link database. The same phenomenon (i.e., resource competition) could arise for the optical regeneration modules. Therefore, a last verification test is performed in the regenerating nodes to ensure that the requested regenerator modules are still available.

VI. GMPLS Protocol Extensions With Regeneration

In Ref. [1], GMPLS protocol extensions were proposed to include routing ($P_{design,l}$, $P_{margin,l}$, $P_{channel,l}$, and $P_{l\ t}$, $OSNR_l$) and signaling information (i.e., β, $C_{adaptation}$) in transparent networks. However, in the case of translucent
networks, additional extensions are required to take into account the regeneration information and to facilitate the application of the power adaptation process. We recall here that $P_{design,l}$ represents the total power budget allocated to link l at the design phase [1], and $P_{margin,l}$ represents the difference between $P_{max\ ,l}$ and $P_{design,l}$.

In the next sub-sections, we provide detailed descrip-tions and encoding formats for the proposed extensions to the OSPF-TE and RSVP-TE protocols. Moreover, we present through an example the routing and signaling mechanisms used to exploit them

A. OSPF-TE

During path computation, optical regeneration sites are usually assigned when the path is not physically feasible. However, this assignment process requires a prior knowledge of the regeneration module sites (i.e., in which node), their capabilities (e.g., acceptable bit rates, modulation for-mats, etc.) and availability, and lastly, their connectivity in the optical nodes (i.e., input/output port connectivity). In this respect, the RFC standard in Ref. [14] proposed several encoding formats to facilitate the dissemination of node in-formation and, particularly, the regeneration information.

In fact, the OSPF-TE protocol allows the dissemination of two types of information: node and link information. Usually, these two kinds of information are disseminated using two top-level type/length/value (TLV): the Optical Node Property TLV and the Link TLV. The information concerning the optical node can be separated into two categories [18]: node devices (e.g., optical regenerators) and switching capabilities of the node (i.e., connectivity matrix) [19]. Thus, depending on the used control plane implementation and on the switching capability of the reconfigurable optical add-drop multiplexers (ROADMs), the connectivity matrix information may be optional. In this work, for simplicity of explanation, we suppose that the ROADMs support

sym-metric switching (complete port-to-port connectivity), and thus there is no need to advertise their internal connectivity. Therefore, we consider only the information concerning optical devices in the ROADMs. The Optical Node Property TLV includes node properties and signal compatibility constraints. The RFC standards in Ref. [20] defined five sub-TLVs to describe these properties and constraints:

1) Resource Block Information,
2) Resource Accessibility,
3) Resource Wavelength Constraints,
4) Resource Block Pool State,
5) Resource Block Shared Access Wavelength Availability.

These five sub-TLVs represent, respectively: the re-source signal constraints and processing capabilities of a node, the structure of the resource pool (i.e., optical regen-erator pool) in relation to the switching devices in the node, the input or output wavelength ranges (for wavelength converter devices), the usage state of a resource (i.e., the availability of an optical regenerator), and lastly, the acces-sibility via shared fibers. For simplification reasons, we suppose that there are sufficient optical ports and switch-ing modules to handle all wavelength signals. Therefore, only the Resource Block information and the Resource Block Pool State are required, and there is no need to ad-vertise the rest of the proposed sub-TLVs.

On one hand, the ResourceBlockInfo sub-TLV allows us to list the optical regenerators existing in the optical nodes and enables the description of their processing capabilities (e.g., acceptable bit rates, modulation formats, types of regenerator: 1R, 2R, 3R, etc.). On the other hand, the Resource Block Pool State allows for having updated information on the regenerators' availability in each node after the establishment of any LSP. Hence, to take into account this information, we propose here to add two new sub-TLVs to the opaque link state advertisement (LSA) type 1 ("Traffic Engineering LSA") in the TE Node Attribute TLV (type 6). The encoding of these sub-TLVs is presented in Ref. [14].

In this work, we consider only the 3R regeneration (sig-nal amplification, pulse shaping, and timing regeneration). Therefore, the first sub-TLV, which is called the RB Set Field, includes the identifier ranges for the 3R regeneration modules in every node. Its encoding description is presented in Ref. [14]. In our case, we suppose that there is only one range defined per node, and thus the sub-TLV can be encoded on 8 bytes: the first 4 bytes encode the identifier for the start of the range, and the last 4 bytes encode the identifier of the end of the range. Moreover, 4 additional bytes are used to indicate the processing capabilities of the regeneration modules (i.e., to indicate that the regeneration type is 3R). The encoding description is also presented in Ref. [14].

The second sub-TLV includes the state of regenerator modules in the form of a bitmap to identify whether the requested regenerator module is available or used. This sub-TLV has a variable length since it depends on the number of regeneration modules in the node, but it must be a multiple of 4 bytes (with padding bits if required). Each bit from the sub-TLV indicates the usage status for a regeneration module (0 for available and 1 for used). The sequence of the bitmap is ordered according to the identifier sequence, defined in the RB Set Field (i.e., the first bit of the bitmap sub-TLV corresponds to the first regeneration module in the regenerator list of the RB Set Field sub-TLV). These OSPF-TE extensions, in addition to those previously proposed in Ref. [1] for link parameters, represent the total information required by any node to execute the Path Computation Algorithm proposed in Section V.

B. RSVP-TE Extensions

In Ref. [1], we conveyed through the RSVP-TE Path mes-sage the required connection information to establish a transparent optical channel. This RSVP-TE Path message includes information on: the central frequency (i.e., channel label), the channel width, and the $C_{adaptation,p}$ parameter. These parameters were valid for an end-to-end connection in a transparent optical network. However, in translucent networks, since optical regenerations are performed, the same information is required for every transparent segment constituting an optical path. Thus, additional information is also required to indicate the need to regenerate the optical signal in intermediate nodes.

1) Label Encoding: We propose to use the Flexi-Grid Label in the Label ERO sub-object as in Ref. [21]. The en-coding of the Flexi-Grid Label is presented in Ref. [22]. This label is used to encode the central frequency and the width (i.e., reserved spectrum bandwidth) of the optical channel. In this work, we suppose that the optical channel keeps the same Flexi-Grid Label all over the path, even if the optical channel is regenerated in intermediate nodes (i.e., we do not take into account the functionality of changing wave-length). This assumption was considered to simplify our routing algorithm and focus on the effect of the optical power control. Therefore, the added labels in the ERO sub-object are the same before and after the identifiers of the regeneration nodes. Once the following extensions are specified under these assumptions, the move to wavelength conversion will be straightforward.

2) Extension for $C_{adaptation}$: After the execution of the Path Computation Algorithm in the ingress node, the required β and $C_{adaptation}$ parameters are available to be ap-plied over the set of segments constituting the regenerated optical path. We propose to create 8-byte sub-TLVs (2 bytes for type, 2 bytes for length, 2 bytes to encode the value of β, and 2 bytes to encode the value of $C_{adaptation}$) in the ERO Hop Attributes sub-object (type 35) in the form of Hop Attributes TLVs [23]. Indeed, multiple Hop Attributes TLVs may be added, depending on the number of hops of the optical path (i.e., proportional to the number of nodes in the path). However, the added Hop Attributes TLVs should have the same value per transparent segment; in contrast, they can have different values between the different transparent segments.

3) Regeneration Encoding: In the case of a non-feasible optical path, a search for available regeneration modules in intermediate nodes is performed by the path computation algorithm. This is possible thanks to the regeneration module availability information disseminated by the OSPF-TE extensions proposed in Section VI.A. Once the optical regeneration modules are chosen through the Regeneration Algorithm, their identifiers should be conveyed through RSVP-TE Path message in order to request their activation in the corresponding nodes.

Therefore, we propose to use the extension Resource-BlockInfo sub-TLV as defined in Ref. [15]. In our case, we encode this extension in the form of 8-byte sub-TLVs (1 byte for type, 1 byte for length, 4 bytes to encode the re-generator identifier, and 2 bytes padded with zeros to en-sure four-octet alignment of the sub-TLV) and put it in the ERO Hop Attributes sub-object (type 35) in the form of Hop Attributes TLVs. The number of added ResourceBlockInfo sub-TLVs (which we call hereafter the "Regeneration" extension) depends on the number of signal regenerations to be performed over the optical path. These extensions include the identifiers of the assigned regeneration modules, and they are proposed with respect to the recommendations of the RFC standard in Ref. [15].

C. Connection Establishment Example

To understand the provisioning process with power adap-tation in a translucent optical network, we consider here, as an example, an optical network with six optical nodes (i.e., ROADMs). Figure 4 shows the six interconnected nodes (A, B, C, D, E, and F). We assume that optical link design has already been performed for all network links, and that every node database is filled with the existing links (spec-

trum bitmap, $P^{opt}_{channel,l}$, $P_{design,l}$, $P_{margin,l}$, $OSNR_l$, and P_l t) and nodes (RB Set Field, regenerator availability bitmap) information. Moreover, we suppose that a connection request between ROADMs F and C is sent to Node F. Figure 5 shows the signaling mechanism and the RSVP-TE message flow triggered to establish the optical channel.

In fact, upon receipt of the connection request by Node F, the Path Computation Algorithm is triggered. We assume that, after performing the algorithm, the selected path p is F-A-B-C (shortest path). We assume also that a set of S free available slots is found, respecting the continuity and contiguity constraints along this path. We suppose also that path p is not transparently feasible, because its

$OSNR_{est,FABC}$ is below the acceptable $OSNR_{min}$, and thus, Node B is assigned to perform signal regeneration. The regeneration in Node B was chosen with respect to the minimum regeneration strategy described in Section IV (i.e., using the Traditional Regeneration Algorithm). In this respect, the optical path is decomposed into two trans-

parent segment F-A-B and B-C, where $OSNR_{est,FAB}$ and $OSNR_{est,BC}$ are higher than $OSNR_{min}$. In this case, the optical channel is power adaptable over the two segments, and a $C_{adaptation}$ parameter is computed per segment ($C_{adaptation,FAB}$ and $C_{adaptation,BC}$).

Before triggering the RSVP-TE signaling process, Node F performs slot and power verification tests over its out-going link (i.e., FA). These tests are executed to ensure that optical spectrum resources are still available and no power saturation will occur after adding the new optical channel over link AB (P_{FA} t $P^{opt}_{channel,FA}$ / $C_{adaptation,FAB}$ ≤ $P_{design,FA}$ $P_{margin,FA}$).

Once the verification is done, Node F sends an RSVP-TE Path message to Node A, including the information on the selected path p, the S slots used, the identifier of the regeneration module, and the $C_{adaptation}$ parameter values (i.e., $C_{adaptation,FAB}$ and $C_{adaptation,BC}$). These parameters are added in ERO in the form of a list of sub-objects, as pro-posed in Section VI.B and respecting the processing of the ERO in Ref. [24]. Figure 5 shows the main parameters of the RSVP-TE message sent to Node A. Upon reception of the Path message by Node A, the same tests are performed over its outgoing link, AB [it checks that S is still avail-able over the link AB and that P_{AB} t $P^{opt}_{channel,AB}$ / $C_{adaptation,FA}$ ≤ $P_{design,AB}$ $P_{margin,AB}$]. After this verification is done, Node A sends a Path message to Node B after processing the ERO as specified in Ref. [24].

Once Node B receives the Path message from Node A, it detects the "Regeneration" extension in the ERO sub-object and thus checks whether the requested regenerator is still available or if it is already assigned to another connection. If it is available, the slot and power verification tests are per-formed over its outgoing link BC (it checks that S is still available over the link BC and that P_{BC} t $P^{opt}_{channel,BC}$ / $C_{adaptation,BC}$ ≤ $P_{design,BC}$ $P_{margin,BC}$). At the end of this step, Node B sends a new Path message to Node C.

Once the Path message arrives at the egress Node C, a hardware configuration is performed for its drop port to receive the optical channel. Moreover, the spectrum bitmap and the power value of the link BC are updated (P_{BC} t P_{BC} t $P^{opt}_{channel,BC}$ / $C_{adaptation,BC}$) in its local database, then a Resv message is sent to Node B.

At reception of Resv message by Node B, slot availability and power verification tests are performed again over link BC (this test is not necessary in case a local resource reservation was made during downstream signaling). Then, a hardware configuration is made to the requested regenerator and the required power attenuation is applied at the input of the transmitter. Moreover, the spectrum bitmap, the regeneration availability bitmap, and the power value of link BC are updated in its local database, and a Resv message is sent to Node A.

In turn, Node A executes the same tests over link AB after the receipt of the Resv message, and once verification is done, a last Resv message is sent to Node F. These tests are repeated in Node F after the reception of the Resv mes-sage. Then, a hardware configuration is performed to its add port and a power adaptation is applied to the transmit-ter. Moreover, the spectrum bitmap, the regenerator availability bitmap, and the power value of link FA (P_{FA} t P_{FA} t $P^{opt}_{channel,FA}$ / $C_{adaptation,FA}$) are updated in its local database. Finally, the optical channel is established, and a connection setup confirmation is sent back to the requester (e.g., network operator or client device).

It is important to note that every optical node sends to its neighboring nodes a set of OSPF-TE advertisements. These advertisements are sent to regularly update other nodes with the changes over its outgoing links, typically after the end of a signaling phase. In our case, additional advertisements are sent to update the changes in optical nodes (i.e., to update the availability of optical regeneration modules in each node).

VII. Simulation and Results

A. Simulation Setup and Scenarios

In order to evaluate the proposed power control process in a translucent network, we improved our distributed

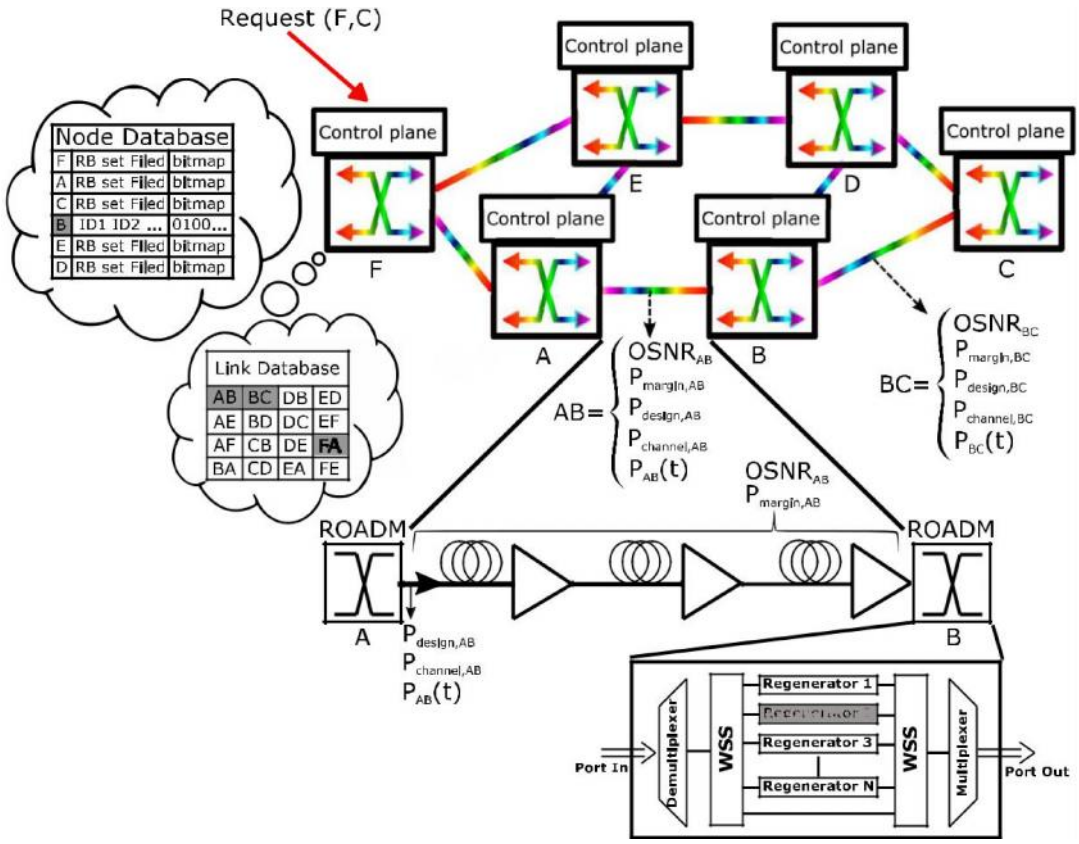

Fig. 5. Flow diagram in F, A, B, and C controller during the connection provisioning process

GMPLS-based network simulator to take into account the optical regeneration. The simulator was extended by adding the newly proposed OSPF-TE and RSVP-TE proto-col extensions in Section VI. The new routing algorithm and the signaling mechanism are implemented as ex-plained in Sections VI.C and V. Moreover, the simulator takes as input a network topology (links, spans, and ampli-fier types), and it designs its optical links using our design method presented in Ref. [25]. Finally, it fills in the OSPF-TE database the essential needed parameters (link

spectrum bitmap, $P^{opt}_{channel,l}$, $P_{design,l}$, $P_{margin,l}$, $OSNR_l$, P_l t , regenerator availability bitmap, RB set field).

Simulations are performed over the European backbone network [26] (32 optical nodes and 42 optical links) assuming same link parameters (CD, alfa, non-linearity coefficient, etc.) and same amplifier portfolio as in Ref. [1]. However, in order to ease result analysis, only 100 Gbit/s optical channels are established in all scenarios (T 100 Gbit⁄s). The filtering penalties resulting from passing through an optical node are 0.05 dB for the 50 GHz channel spacing (four slots of 12.5 GHz) and 0.64 dB for the 37.5 GHz (three slots of 12.5 GHz) [27].

The minimum accepted OSNR at the receiver side, using 0.1 nm noise reference bandwidth, including operational margins, is set to 15 dB for a 100 Gbit/s quadrature phase-shift keying (QPSK) modulation format with coherent detection and soft decision forward error correction (FEC), whatever the channel bandwidth (three or four slots of 12.5 GHz). Eight scenarios are considered. We tagged with “PAPV” the scenarios using the power control and power margins in their control plane.

- Fixed-grid with optical regeneration (FG_R): this scenario represents today’s translucent optical networks. For each channel, the spectral occupation is four slots over each transparent segment.
- Fixed-grid with power control, power margins, and optical regeneration (FG4S_PAPV_R): this scenario is the same as FG_R but with power control. The power adaptation is applied for the minimum acceptable OSNR value.

Flex-grid with optical regeneration (FX_R): this scenario is the same as FG_R but with channels that occupy each, only three contiguous slots over every transparent segment

- Flex-grid with power control, power margins, and optical regeneration (FX3S_PAPV_R): this scenario is the same as FX_R but with channel power adaptation.
- Flex-grid with optical regeneration (FX3-4S_R): this scenario is a mix of a fixed-grid and flex-grid network. The Path Computation Algorithm first tries three slots of 12.5 GHz for the channel setup. If the path is not transparently feasible, the algorithm tries to establish the optical channel using four slots. If still unfeasible, an optical node is assigned for signal regeneration. This regeneration is performed considering a four-slot channel.

- Flex-grid with power control, power margins, and optical regeneration (FX3-4S_PAPV_R4): this scenario is the same as FX3-4S_R but with power control and with the same regeneration strategy.

- Flex-grid with power control, power margins, and optical regeneration (FX3-4S_PAPV_R3): this scenario is the same as FX3-4S_PAPV_R4. However, contrarily to the previous scenario (FX3-4S_PAPV_R4), this regeneration is performed using a three-slot channel.
- Flex-grid with unlimited link power resources and optical regeneration (FX3S_Full_R): this is a benchmark scenario. It is an ideal (unrealistic) scenario, which is considered to evaluate the power saturation problem. In this scenario, only three-slot channels are established, and the P_{max} ,l of every link l is supposed to be unlimited.

In this work, we consider the same link design as in Ref. [1], and the full usable bandwidth of each link is set to 4.8 THz (optical amplifier usable bandwidth) as defined by the ITU-T. Table I summarizes the eight simulated scenarios. The Path Computation Algorithm presented in Section V is modified to enable the simulation of the different scenarios. Depending on the scenario, some tests are activated or deactivated. In the algorithm, only one shortest path is computed for any request between any node pairs (s, d). The connection request is blocked if it cannot pass the set of tests (continuity, contiguity, physical feasibility, and, if needed, power feasibility). Once all the tests are passed, the provisioning process is triggered with a set of channel parameters (path, slots, one or multiple $C_{adaptation}$ coefficients, and regenerator identifiers).

B. Simulation Configurations

Scenarios were simulated considering a dynamic connection establishment, where optical connections are established and released automatically. Connection requests are dynamically generated following a Poisson process, where every source-destination pair of each request is randomly chosen among all network nodes according to a uniform distribution. The inter-arrival and holding times for every request follow an exponential distribution with aver-ages of $1/\lambda$ and $1/\mu$, respectively. The connection holding time $1/\mu$ is fixed to 100 s. The offered network load is obtained by varying $1/\lambda$. The processing time of the packets is considered negligible compared to the propagation delays.

For each network load (i.e., for every value of $1/\lambda$), thirty simulation runs (each run with a different seed) are per-formed for each of the eight scenarios. Simulation results are collected after the arrival of 35×10^4 requests in order to ensure that the network is in a stable state. The results depicted in the following figures are given by averaging the 30 simulation runs of each $1/\lambda$ with a confidence interval of 95% (too small to be displayed on the figures). It is important to note that, for every scenario, the same 30 seeds are used in order to exactly simulate the same sequence of optical connection requests. Moreover, for the purpose of the study, the number of 3R regeneration modules per node is not considered as a constraint, and thus, no blocking could occur due to the unavailability of regeneration modules.

C. Simulation Results

We consider the blocking probability (BP) as an evaluation criterion. It is expressed as the ratio between the number of blocked light paths and the number of requested light paths. Simulation results for blocking probability are plotted as a function of the total network load defined as $N \times \lambda/\mu$, where N 32 is the number of network nodes, and the load is expressed in Erlang.

Figure 6 shows the blocking probability of the eight scenarios as a function of network load. All scenarios with power adaptation (i.e., FG4S_PAPV_R, FX3S_PAPV_R, FX3-4S_PAPV_R4, and FX3-4S_PAPV_R3) have lower BP than the other scenarios (i.e., FG_R, FX_R, and FX3-4S_R). We can notice that, the FG_R, FX_R, and FX3-4S_R scenarios have approximately the same blocking probability. These scenarios are limited by the maximum number of channels designed for optical links or by spectrum unavailability. In fact, the use of flex-grid technology in FX_R and FX3-4S_R (three-slot channels) reduces the spectrum occupation in optical links. However, even if there are spectrum slots available, blocking may arise from the limited number of channels per link (the number of channels is limited to avoid power saturation since the control plane is not power aware). Accordingly, the blocking reason in FX_R is more likely to be due to the limitation of the number of channels, where it is limited to 80 per link. However, in FX3-4S_R, the blocking occurs due to the spectrum fragmentation and to the limitation of number of channels, since mixing between three and four slots creates unusable spectrum slots. This analysis is confirmed in the next section when the blocking reasons are analyzed.

In contrast, the performance of the FG4S_PAPV_R, FX3S_PAPV_R, FX3-4S_PAPV_R4, and FX3-4S_PAPV_R3 scenarios is impacted differently. In these scenarios, an additional type of blocking may arise, which is the power saturation. For example, the FG4S_PAPV_R scenario shows that the use of power adaptation while keeping in use the fixed-grid technology helps increase the performance of the network. This increase is achieved through power saving, allowing the establishment of more than 80 channels per link. However, this gain is directly limited by the spectrum occupation due to the use of four slot channels, promoting, in this respect, more blocking due to spectrum unavailability. It can be noted also that the use of flexible technology with power adaptation offers better performance in terms of blocking probability. Indeed, the FX3S_PAPV_R, FX3-4S_PAPV_R, and FX3-4S_PAPV_R3 scenarios undergo less blocking due to the use of three slot channels, reducing the spectrum occupation in optical links. These scenarios benefit at the same time from the spectrum occupation reduction and from power saving.

D. Blocking Reasons Analysis

As in Ref. [1], we complete our study with a deep analysis of the blocking reasons in each scenario. To this end, we plotted the reasons of request blocking for each scenario in bar charts. The same blocking reasons presented in Ref. [1] are considered (No Spec, No OSNR, No Pow, and MXCE). The No Spec reason represents blocking due to the unavailability of spectrum slots for a connection re-quest. The No Pow reason represents blocking due to the unavailability of sufficient power resources. The MXCE reason represents blocking when the number of channels exceeds the one authorized over optical links (used for scenarios with no power awareness, such as FG_R). Finally, the No OSNR reason represents the blocking when there is no physically feasible path.

However, it cannot exist any-more, since optical regeneration can be performed.

The blocking counting method is described as follows: for each connection request and its computed path p, if there are no available continuous and contiguous slots that satisfy the connection request, the blocking reason is counted as No Spec. Contrariwise, in the case the spectrum resources are available, the blocking reason is counted as No Pow or as MXCE depending on the scenario. For FG_R, FX_R, and FX3-4S_R scenarios, because no power control is per-formed, the MXCE blocking reason is considered when the number of channels established over any link exceeds the maximum allowed (i.e., number of channels >80). For the other scenarios with power awareness, the blocking reason is counted as No Pow. In summary, the priority is given to the No Spec blocking and then to the No Pow and MXCE. This counting method allows avoiding confusion on the No Pow blocking.

To fairly compare for all scenarios, we recorded per scenario the blocking reasons for the 10,000 connection requests generated after the first 35×10^4 requests (same request sequence, same traffic, and same set of source and destination node pairs for all scenarios). Then, we plotted the number of blocked requests per blocking reason for each of the eight scenarios. Figure 7 shows the number

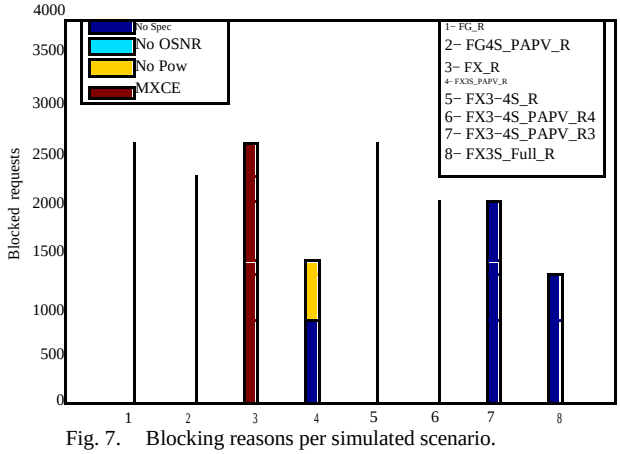

Fig. 7. Blocking reasons per simulated scenario.

of blocked requests in every scenario at a network load of 600 Erlang (where BP > 0.1).

We can notice that at this load (i.e., 600 Erlang) the scenarios without power adaptation, like FG_R, FX_R, and FX34_R, have approximately the same number of blocked requests. In FG_R and FX3-4S_R, two reasons for blocking occur: No Spec and MXCE. However, in the FX_R scenario, the blocking is only due to MXCE, since the use of three slot channels reduces the spectrum occupation in every link, and thus, the spectrum is no longer a serious limitation. This shows the impact of not consider-ing link power resources (high number of blocked requests due to MXCE).

In FG4S_PAPV_R, FX3-4S_PAPV_R4, and FX3-4S_PAPV_R3, the blocking is due only to No Spec because of two reasons: there is no more limitation to the number of channels per link, and the power adaptation process was able to save the required power for the additional channels. However, even if the quantity of saved power is reduced due to the use of three slot channels in FX3-4S_PAPV_R4 and FG3-4S_PAPV_R3, only No Spec blocking is arising since the mixing of three- and four-slot channels increases the fragmentation of the optical spectrum.

Contrariwise, the FX3S_PAPV_R scenario is more impacted due to the use of three slot channels (which reduces the quantity of saved optical power because of the high filtering penalty). Therefore, the No Pow blocking appears in addition to the No Spec, because the link spectrum is less fragmented (i.e., only horizontal fragmentation exists), and thus optical links can be more loaded. Finally, as expected in FX3S_Full_R, only No Spec blocking is arising because link power resources are supposed to be unlimited. These results demonstrate that the use of the power adaptation process allows reduction of the number of blocked requests and thus increases network capacity and performance.

In summary, the results in Figs. 6 and 7 demonstrate that upgrading the network with flex-grid technology with-out adapting channels power prevents us from benefiting from the reduction in spectrum occupation (as it was shown with FX_R and FX3-4S_R). Therefore, a power-aware control plane with power adaptation process helps to increase network capacity and thus to reduce the blocking probability as in FG4S_PAPV_R. Indeed, when flexibility is associated with power adaptation, as in FX3S_PAPV_R, FX3-4S_PAPV_R4, and FX3-4S_PAPV_R3, we can get better network performance and an important increase in network capacity.

E. Performance in Terms of Optical Regeneration

In terms of regeneration, each scenario performs a smaller or larger number of optical regenerations depend-ing on the regeneration strategy used in the Path Computation Algorithm. Figure 8 shows the number of optical regeneration modules used in the eight scenarios as a function of network load. It can be noticed that the scenarios using four-slot channels (such as FG_R, FG4S_PAPV_R, FX3-4S_R, FX3-4S_PAPV_R4, and FX3-4S_PAPV_R3) use less optical regeneration modules com-pared with the scenarios using only three slot channels. Indeed, the three-slot channels suffer from a high filtering penalty, and thus long-reach channels are more likely to be regenerated in a higher number of intermediate nodes.

Moreover, it can be noticed also on Fig. 8 that these scenarios (FG_R, FG4S_PAPV_R, FX3-4S_R, and FX3-4S_PAPV_R4, except FX3-4S_PAPV_R3) use on aver-age the same number of regenerators. This result indicates that even with the establishment of additional channels in scenarios using the power adaptation process (i.e., FG4S_PAPV_R and FX3-4S_PAPV_R4), the number of used regenerators is still the same in comparison with the scenarios without the power adaptation process. This means that the use of the power adaptation process allows an increase in the capacity of the network for the same cost in terms of regeneration. This effect can be explained through Fig. 9, where we plotted in bar charts the number of blocked requests per number of hops.

Figure 9 shows that the number of long-reach requests in FG4S_PAPV_R and FX3-4S_PAPV_R4 are more likely

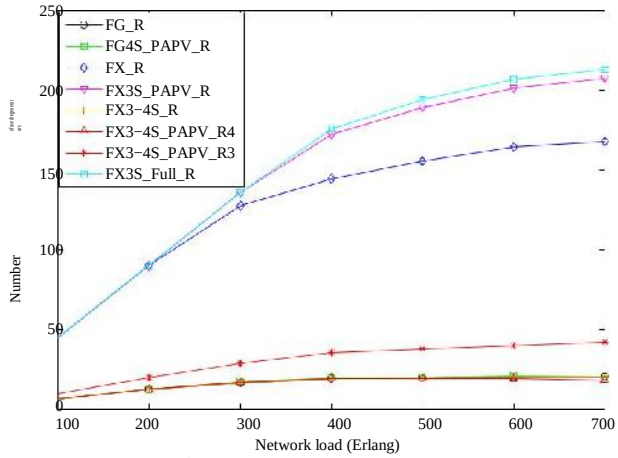

Fig. 8. Total number of used regenerators in the network per sce-nario as a function of network load.

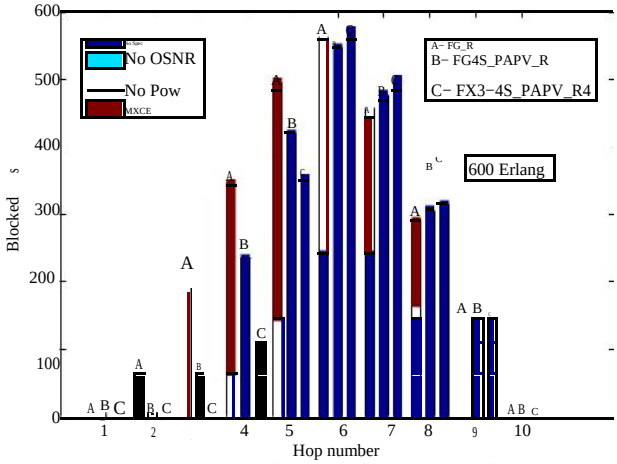

Fig. 9. Blocked requests as a function of the number of hops.

to be blocked in comparison with the FG_R scenario. In fact, the establishment of more than 80 channels per link increases the spectral occupation in optical links, and thus long-reach channels are blocked due to the horizontal fragmentation. At the same time, when mixing three- and four-slot channels in FX3-4S_PAPV_R4, additional blocking could occur due to the vertical fragmentation. This is why the average number of regenerators used in FX3-4S_PAPV_R4 is slightly smaller than in FG4S_PAPV_R (long-reach channels are more blocked in FX3-4S_PAPV_R4, therefore less regenerators are used).

However, Fig. 8 shows that the FX3-4S_PAPV_R3 scenario uses more optical regenerators compared to FX3-4S_PAPV_R4. In fact, two reasons are behind this result. The first one is because performing optical regeneration with three slot channels helps to reduce spectrum occupation, and thus more optical channels can be established in the network. The second one is because in FX3-4S_PAPV_R3 the non-feasible channels are regenerated using three slots, and thus, due to the high filtering penalty, more optical regeneration modules can be required along the regenerated path. Finally, it can be remarked that in FX3S_PAPV_R there are more optical regenerators used on average in comparison to FX_R. This is expected, since a higher number of channels is established when the power adaptation process is used.

VIII. Conclusion

In this paper, we addressed the optical power adaptation in translucent optical networks. We extended the GMPLS protocol suite in order to support optical regeneration and the power adaptation process. In this respect, a Path Computation Algorithm with new protocol extensions and signaling mechanisms was proposed to RSVP-TE and OSPF-TE protocols. These extensions allow taking into account the optical regenerator availability and assignment as well as performing channel power adaptation. Moreover, the migration from fixed-grid to flex-grid net-works was studied with dynamic traffic patterns, where it was demonstrated that the power saturation problem can arise independently from the traffic pattern (i.e., incremental [1] or dynamic).

Simulation results showed that upgrading a fixed-grid network with flexible technology without adapting channel power prevents us from benefiting from spectrum saving and increases network cost. Moreover, it showed that the regeneration assignment strategy used in the Path Computation Algorithm can also impact the performance of the network and its cost. Finally, the usage of appropriate regeneration algorithms by network operators allows significant increase in their network capacity [28].

It is important to note that this work on power control is not meant to be limited to the GMPLS control plane. The same principle of optical power control and optimized regeneration placement can be implemented on software defined network (SDN) controllers via other suitable proto-cols. This can be realized by simply adding the same pro-posed parameters in its corresponding protocol extensions for the considered control plane. Moreover, including all flexibility parameters (such as modulation format, baud rate, and others) in the routing algorithm would improve the usage of network resources. This increases its capacity and could even increase the optical power issue. Therefore, proposing a better routing algorithm is left for future works.

References

[1] M. Kanj, E. L. Rouzic, J. Meuric, B. Cousin, and D. Amar, “Optical power control in GMPLS control plane,” J. Opt. Commun. Netw., vol. 8, no. 8, pp. 553–568, Aug. 2016.

[2] R. Martinez, R. Casellas, R. Munoz, T. Tsuritani, and T. Otani, “Experimental GMPLS routing for dynamic provisioning in translucent wavelength switched optical networks,” in Conf. Optical Fiber Communication, Mar. 2009, pp. 1–3.

[3] R. Martinez, R. Casellas, R. Munoz, and T. Tsuritani, “Experimental translucent-oriented routing for dynamic lightpath provisioning in GMPLS-enabled wavelength switched optical networks,” J. Lightwave Technol., vol. 28, no. 8, pp. 1241–1255, Apr. 2010.

[4] N. Sambo, A. Giorgetti, F. Cugini, N. Andriolli, L. Valcarenghi, and P. Castoldi, “Accounting for shared regenerators in GMPLS-controlled translucent optical networks," J. Lightwave Technol., vol. 27, no. 19, pp. 4338–4347, Oct. 2009.

[5] H. Guo, T. Tsuritani, S. Okamoto, and T. Otani, “Demonstration of GMPLS-controlled inter-domain transpar-ent optical networks,” in 34th European Conf. Optical Communication, Sept. 2008, pp. 1–2.

[6] R. Martinez, C. Pinart, F. Cugini, N. Andriolli, L. Valcarenghi, P. Castoldi, L. Wosinska, J. Comellas, and G. Junyent, “Challenges and requirements for introducing impairment-awareness into the

management and control planes of ASON/GMPLS WDM networks," IEEE Commun. Magazine, vol. 44, no. 12, pp. 76–85, Dec. 2006.

[7] Y. Lee, G. Bernstein, and W. Imajuku, "Framework for GMPLS and PCE control of wavelength switched optical net-works (WSON)," IETF RFC 6163, Apr. 2011.

[8] F. Cugini, N. Sambo, A. Giorgetti, L. Valcarenghi, P. Castoldi, E. L. Rouzic, and J. Poirrier, "GMPLS extensions to encom-pass shared regenerators in transparent optical networks," in 33rd European Conf. and Exhibition of Optical Communication, Sept. 2007, pp. 1–2.

2 N. Sambo, F. Cugini, N. Andriolli, A. Giorgetti, L. Valcarenghi, and P. Castoldi, "Lightweight RSVP-TE extensions to account for shared regenerators in translucent optical networks," in Photonics in Switching, Aug. 2007, pp. 35–36.

3 N. Sambo, N. Andriolli, A. Giorgetti, F. Cugini, L. Valcarenghi, and P. Castoldi, "Distributing shared regenera-tor information in GMPLS-controlled translucent networks," IEEE Commun. Lett., vol. 12, no. 6, pp. 462–464, June 2008.

4 D. J. Ives, P. Bayvel, and S. J. Savory, "Adapting transmitter power and modulation format to improve optical network performance utilizing the Gaussian noise model of nonlinear impairments," J. Lightwave Technol., vol. 32, no. 21, pp. 4087– 4096, Nov. 2014.

5 A. Nag, M. Tornatore, and B. Mukherjee, "Power manage-ment in mixed line rate optical networks," in Integrated Photonics Research, Silicon and Nanophotonics and Photonics in Switching, Optical Society of America, 2010, pa-per PTuB4.

6 D. J. Ives, P. Bayvel, and S. J. Savory, "Assessment of options for utilizing SNR margin to increase network data through-put," in Optical Fiber Communication Conf., Optical Society of America, 2015, paper M2I.3.

7 G. Bernstein, Y. Lee, D. Li, W. Imajuku, and J. Han, "Routing and wavelength assignment information encoding for wave-length switched optical networks," IETF RFC 7581, June 2015.

8 G. Bernstein, S. Xu, Y. Lee, G. Martinelli, and H. Harai, "Signaling extensions for wavelength switched optical networks," IETF RFC 7689, Nov. 2015.

9 Y. Lee, G. Bernstein, D. Li, and W. Imajuku, "Routing and wavelength assignment information model for wavelength switched optical networks," IETF RFC 7446, Feb. 2015.

10 D. C. Rider, J. C. Slezak, A. V. W. Smith, and A. Lucent, "Regenerators placement mechanism for wavelength switched optical networks," U.S. patent 10097901 (March 3, 2002).

11 F. Zhang, Y. Lee, J. Han, G. Bernstein, and Y. Xu, "OSPF-TE extensions for general network element constraints," IETF RFC 7580, June 2015.

12 G. Bernstein, Y. Lee, D. Li, W. Imajuku, and J. Han, "General network element constraint encoding for GMPLS-controlled networks," IETF RFC 7579, June 2015.

13 Y. Lee and G. Bernstein, "GMPLS OSPF enhancement for sig-nal and network element compatibility for wavelength switched optical networks," IETF RFC 7688, Nov. 2015.

14 L. Berger, "Generalized multi-protocol label switching (GMPLS) signaling resource reservation protocol-traffic engineering (RSVP-TE) extensions," IETF RFC 3473, Jan. 2003.

15 A. Farrel, D. King, Y. Li, and F. Zhang, "Generalized labels for the flexi-grid in lambda switch capable (LSC) label switching routers," IETF RFC 7699, Nov. 2015.

16 C. Margaria, G. Martinelli, S. Balls, and B. Wright, "Label switched path (LSP) attribute in the explicit route object (ERO)," IETF RFC 7570, July 2015.

17 D. Awduche, L. Berger, D. Gan, T. Li, V. Srinivasan, and G. Swallow, "RSVP-TE: extensions to RSVP for LSP tunnels," IETF RFC 3209, Dec. 2001.

18 M. Kanj, E. L. Rouzic, D. Amar, J. L. Auge, B. Cousin, and N. Brochier, "Optical power control to efficiently handle flex-grid spectrum gain over existing fixed-grid network infra-structures," in Int. Conf. Computing, Networking and Communications (ICNC), Feb. 2016, pp. 1–7.

19 G. Bernstein, Y. Lee, D. Li, W. Imajuku, and J. Han, "General network element constraint encoding for GMPLS-controlled networks," IETF RFC 7579, June 2015.

20 Y. Lee and G. Bernstein, "GMPLS OSPF enhancement for sig-nal and network element compatibility for wavelength switched optical networks," IETF RFC 7688, Nov. 2015.

21 L. Berger, "Generalized multi-protocol label switching (GMPLS) signaling resource reservation protocol-traffic engi-neering (RSVP-TE) extensions," IETF RFC 3473, Jan. 2003.

22 A. Farrel, D. King, Y. Li, and F. Zhang, "Generalized labels for the flexi-grid in lambda switch capable (LSC) label switching routers," IETF RFC 7699, Nov. 2015.

23 C. Margaria, G. Martinelli, S. Balls, and B. Wright, "Label switched path (LSP) attribute in the explicit route object (ERO)," IETF RFC 7570, July 2015.

24 D. Awduche, L. Berger, D. Gan, T. Li, V. Srinivasan, and G. Swallow, "RSVP-TE: extensions to RSVP for LSP tunnels," IETF RFC 3209, Dec. 2001.